Fabrication of Micro-Patterned Chip with Controlled Thickness for High-Throughput Cryogenic Electron Microscopy

Min-Ho Kang[1,2], **Minyoung Lee**[3,4], **Sungsu Kang**[3,4], **Jungwon Park**[3,4,5,6]

[1] Department of Biomedical-Chemical Engineering, The Catholic University of Korea [2] Department of Biotechnology, The Catholic University of Korea [3] School of Chemical and Biological Engineering, and Institute of Chemical Processes, Seoul National University [4] Center for Nanoparticle Research, Institute of Basic Science (IBS) [5] Institute of Engineering Research, College of Engineering, Seoul National University [6] Advanced Institutes of Convergence Technology, Seoul National University

Corresponding Author

Jungwon Park
jungwonpark@snu.ac.kr

Citation

Kang, M.H., Lee, M., Kang, S., Park, J. Fabrication of Micro-Patterned Chip with Controlled Thickness for High-Throughput Cryogenic Electron Microscopy. *J. Vis. Exp.* (182), e63739, doi:10.3791/63739 (2022).

Date Published

April 21, 2022

DOI

10.3791/63739

URL

jove.com/video/63739

Abstract

A major limitation for the efficient and high-throughput structure analysis of biomolecules using cryogenic electron microscopy (cryo-EM) is the difficulty of preparing cryo-EM samples with controlled ice thickness at the nanoscale. The silicon (Si)-based chip, which has a regular array of micro-holes with graphene oxide (GO) window patterned on a thickness-controlled silicon nitride (Si_xN_y) film, has been developed by applying microelectromechanical system (MEMS) techniques. UV photolithography, chemical vapor deposition, wet and dry etching of the thin film, and drop-casting of 2D nanosheet materials were used for mass-production of the micro-patterned chips with GO windows. The depth of the micro-holes is regulated to control the ice thickness on-demand, depending on the size of the specimen for cryo-EM analysis. The favorable affinity of GO toward biomolecules concentrates the biomolecules of interest within the micro-hole during cryo-EM sample preparation. The micro-patterned chip with GO windows enables high-throughput cryo-EM imaging of various biological molecules, as well as inorganic nanomaterials.

Introduction

Cryogenic electron microscopy (cryo-EM) has been developed to resolve the three-dimensional (3D) structure of proteins in their native state[1,2,3,4]. The technique involves fixing proteins in a thin layer (10-100 nm) of vitreous ice and acquiring projection images of randomly oriented proteins using a transmission electron microscope (TEM), with the sample maintained at liquid nitrogen temperature. Thousands to millions of projection images are acquired and used to reconstruct a 3D structure of the protein by computational algorithms[5,6]. For successful analysis with cryo-EM, cryo-sample preparation has been automated by plunge-freezing the equipment that controls the blotting conditions, humidity, and temperature. The sample solution is loaded onto a TEM grid with a holey carbon membrane,

successively blotted to remove the excess solution, and then plunge-frozen with liquid ethane to produce thin, vitreous ice[1,5,6]. With the advances in cryo-EM and the automation of sample preparation[7], cryo-EM has been increasingly used to solve the structure of proteins, including envelope proteins for viruses and ion channel proteins in the cell membrane[8,9,10]. The structure of envelope proteins of pathogenic viral particles is important for understanding viral infection pathology, as well as developing the diagnosis system and vaccines e.g., SARS-CoV-2[11], which caused the COVID-19 pandemic. Moreover, cryo-EM techniques have recently been applied to material sciences, such as for imaging beam-sensitive materials used in battery[12,13,14] and catalytic systems[14,15] and analyzing the structure of inorganic materials in solution-state[16].

Despite noticeable developments in cryo-EM and relevant techniques, limitations exist in cryo-sample preparation, hindering high-throughput 3D structure analysis. Preparing a vitreous ice film with optimal thickness is especially important for obtaining the 3D structure of biological materials with atomic resolution. The ice must be thin enough to minimize background noise from electrons scattered by the ice and to prohibit overlaps of biomolecules along the electron beam path[1,17]. However, if the ice is too thin, it can cause protein molecules to align in preferred orientations or denature[18,19,20]. Therefore, the thickness of vitreous ice should be optimized depending on the size of the material of interest. Moreover, extensive effort is typically needed for the sample preparation and manual screening of ice and protein integrity on the prepared TEM grids. This process is extremely time-consuming, which hinders its efficiency for high-throughput 3D structure analysis. Therefore, improvements in the reliability and reproducibility of cryo-EM sample preparation would enhance the utilization of cryo-EM in structural biology and commercial drug discovery, as well as for material science.

Herein, we introduce microfabrication processes for making a micro-patterned chip with graphene oxide (GO) windows designed for high-throughput cryo-EM with controlled ice thickness[21]. The micro-patterned chip was fabricated using microelectromechanical system (MEMS) techniques, which can manipulate the structure and dimensions of the chip depending on the imaging purposes. The micro-patterned chip with GO windows has a microwell structure that can be filled with the sample solution, and the depth of the microwell can be regulated to control the thickness of the vitreous ice. The strong affinity of GO for biomolecules enhances the concentration of biomolecules for visualization, improving the efficiency of the structure analysis. Furthermore, the micro-patterned chip is composed of an Si frame, which provides high mechanical stability for the grid[19], making it ideal for handling the chip during sample preparation procedures and cryo-EM imaging. Therefore, a micro-patterned chip with GO windows fabricated by MEMS techniques provides reliability and reproducibility of cryo-EM sample preparation, which can enable efficient and high-throughput structure analysis based on cryo-EM.

Protocol

1. Fabrication of micro-patterned chip with GO windows (Figure 1)

1. Deposit the silicon nitride.
    1. Deposit low-stress silicon nitride (Si_xN_y) on both sides of the Si wafer (4 inch diameter and 100 µm thickness) using low-pressure chemical vapor deposition (LPCVD) at 830 °C and a pressure of

Copyright © 2022 JoVE Journal of Visualized Experiments

150 mTorr, under a flow of 170 sccm dichlorosilane (SiH_2Cl_2, DCS) and 38 sccm ammonia (NH_3).

2. Using a deposition rate of ~30 Å/min, control the Si_xN_y thickness to be within 25-100 nm by varying the deposition time.

NOTE: Extreme care should be taken when handling the Si wafer because the wafer is very thin and fragile. Take care not to bend the wafer during its handling or loading in the equipment.

2. Pattern the photoresist.

1. Apply a hexamethyldisilazane (HMDS) solution on the Si_xN_y-deposited Si wafer with enough volume to cover the entire surface of the wafer, spin coat with a spin coater at 3,000 rpm for 30 s, and bake at 95°C for 30 s on a hot plate to render the wafer surface hydrophobic and thus ensure a good coating performance with photoresist (PR).

2. Apply positive PR (**Table of Materials**) with enough volume to cover the entire surface of the wafer, spin coat at 3,000 rpm for 30 s, and bake at 100 °C for 90 s on a hot plate. Spin-coated PR has a thickness of 500 nm.

3. Expose the PR-coated wafer with ultraviolet light (365 nm wavelength and 20 mW/cm^2 intensity) for 5 s through a chromium mask (**Figure 2A-D**) using an aligner.

4. Develop the PR for 1 min using a developer (**Table of Materials**) and rinse the wafer by immersing it in deionized (DI) water 2x. Fully dry the PR-patterned wafer by blowing N_2 gas onto the wafer surface.

NOTE: Extreme care should be taken while blowing N_2 gas onto the Si wafer because the wafer is very thin and fragile. Do not blow N_2 gas with high pressure in a direction perpendicular to the wafer, as this may cause the wafer to fracture.

3. Pattern the Si_xN_y.

1. Etch the exposed Si_xN_y following the patterning of the PR using a lab-built reactive ion etcher (RIE), with 3 sccm sulfur hexafluoride (SF_6) gas at a radiofrequency (RF) power of 50 W. The etching rate with these settings is ~6 Å/s. Set the etching time depending on the thickness of the Si_xN_y layer deposited.

NOTE: The etching rate may vary and need in-lab optimization depending on the specifications of the RIE equipment used.

2. Eliminate the PR by immersing the Si_xN_y patterned wafer in acetone at room temperature for 30 min, followed by rinsing the wafer by immersing it in DI water 2x. Fully dry the wafer by blowing N_2 gas onto the wafer surface.

NOTE: Extreme care should be taken while immersing or taking out the wafer from the solutions because the wafer can be fractured by the surface tension of the solution. Do not immerse or take out the wafer parallel to the surface of the solution. Use precision wafer handling tweezers with carbon fiber tips. Do not strongly grab the wafer with the tweezer; lift one side of the wafer until the wafer tilts to an angle, where it can be taken out from the solution. The wafer may fracture when it bends due to the firm grip during lifting.

4. Etch the Si.

1. Prepare a 1.5 M potassium hydroxide (KOH) solution by dissolving KOH powder in DI water at 80 °C.

2. Immerse the Si_xN_y patterned wafer in KOH solution to etch the exposed Si. Leave the wafer in the solution with stirring until the free-standing Si_xN_y windows can be observed at the opposite side of the patterned Si_xN_y.

   NOTE: The wet etching time may differ depending on the thickness of the Si; for a 100 µm thick wafer, wet etching normally takes several hours. Do not set the stirring speed too high during Si etching because the free-standing Si_xN_y windows are very thin and can be fractured by the flow of the fluid. In this experiment, the stirring rate was set to 250 rpm.

3. Clean the etched wafer by dipping it several times in a DI water bath to eliminate etching residues. Dry the wafer in the air.

   NOTE: Extreme care should be taken while immersing or taking out the Si patterned wafer from the solutions because the free-standing Si_xN_y windows are very thin and fragile and can be fractured by the surface tension of the solution. The wafer should be immersed or taken out at an angle, such that the edge of the wafer enters and exits the solution first.

5. Eliminate the KOH etching residues.

   1. Lightly press the boundaries of the chip array with a tweezer to obtain an array of chips that will be micro-patterned (**Figure 1B**).

   2. Prepare 1.5 M KOH solution at 80 °C with stirring.

   3. Immerse the chip array in KOH solution for 30 s and rinse it by dipping it in DI water 2x. Fully dry the chips by blowing N_2 gas.

      NOTE: Extreme care should be taken while dipping the chips in solutions and blow-drying them with N_2 gas because the free-standing Si_xN_y windows are very thin and fragile. While the chip is immersed in KOH solution, stirring should be stopped. The chips should be dipped with their edges first in the direction perpendicular to the solution and blown with N_2 gas in the parallel direction.

   4. Fully dry the chip array in the air for at least 1 h.

6. Pattern the PR.

   1. Prepare a blank 525 µm Si wafer as solid support. Spin coat the Si wafer with HMDS and positive PR, as described above, but attach the chip array (with the free-standing Si_xN_y window side upward) on the Si wafer before baking the PR. The PR acts as an adhesive between the wafer and the chip array. Bake the Si wafer attached with the chip array at 100 °C for 90 s on a hot plate.

   2. Spin coat the chip set with HMDS and positive PR, as described above.

   3. Expose the chip set with ultraviolet light (365 nm wavelength; 20 mW/cm^2 intensity) for 5 s through a chromium mask (**Figure 2E,F**) using an aligner.

   4. Develop the PR using a developer for 15 s, rinse the chip set by dipping it in DI water 2x, and fully dry the PR patterned chip set by blowing N_2 gas.

7. Prepare the micro-patterned Si_xN_y.

Copyright © 2022 JoVE Journal of Visualized Experiments

1. Etch Si_xN_y following the PR patterning using a lab-built RIE, with 3 sccm SF_6 gas at RF power of 50 W. Control the etching time depending on the thickness of the Si_xN_y layer.

8. Eliminate the PR.

    1. Eliminate the PR by immersing the patterned chip set in 1-methyl-2-pyrrolidinone (NMP) solution at 60 °C and leaving it overnight. Rinse the chip set by dipping it in DI water 2x, and fully dry the patterned chip set by blowing N_2 gas.

    2. Eliminate the PR residues with an O_2 plasma process using 100 sccm O_2 gas at RF power of 150 W for 1 min with the lab-built RIE.

9. Rinse the micro-patterned chip.

    1. Prepare 1.5 M KOH solution at 80 °C.

    2. Immerse the micro-patterned chips in KOH solution for 30 s to fully eliminate the PR residues and rinse the chips by immersing them in DI water 2x. Fully dry the chips by blowing N_2 gas.

    3. Fully dry the chips in the air for at least 1 h.

10. Transfer graphene oxide (GO) by the drop-casting method.

    1. Dilute GO solution (2 mg/mL) to 0.2 mg/L with DI water and sonicate for 10 min to break up aggregates of GO sheets. Centrifuge the diluted GO solution at 300 x *g* for 30 s.

    2. Glow discharge the Si-etched side of the micro-patterned chip to render the chip surface with positive charge using a glow discharger (**Table of Materials**) at 15 mA for 1 min.

    3. Drop 3 µL of the GO solution onto the glow discharged side of the micro-patterned chip and leave the drop on the chip for 1 min. After 1 min, blot away the excess GO solution on the chip with filter paper.

    4. Wash the GO-transferred chip with DI water droplets prepared on paraffin film and blot away the DI water on the chip with filter paper. Repeat this procedure 2x on the GO transferred side and 1x on the opposite side. Dry the GO-transferred chip at room temperature overnight.

    5. Wash the micro-patterned chip with GO windows by immersing it in the DI water and blow-dry the chip with N_2 gas.

2. Cryo-EM imaging

1. Prepare the cryo-sample.

    1. Prepare the cryo-sample using a mechanical cryo-plunging machine (**Table of Materials**), which controls the temperature, humidity, blotting time, and force. After loading the blotting pad onto the blotters, ensure that the humidity and the temperature in the chamber are maintained at 100% and 15 °C, respectively.

    2. Pick up the micro-patterned chip with a typical cryo-tweezer and load the tweezer to the cryo-plunging machine. Pipet 3 µL of sample solution onto the micro-patterned chip at the hole-patterned side, with GO windows on the bottom. Control the blotting time and force depending on the sample solution.

    NOTE: Here, biological specimens, namely human immunodeficiency virus (HIV-1), ferritin, proteasome 26S, groEL, apoferritin protein particles, and tau

filament proteins were used for cryo-EM imaging. In addition, diverse types of inorganic materials, such as Fe_2O_3 nanoparticles (NP), Au nanoparticles, Au nanorods, and silica nanoparticles, were used for cryo-EM imaging. The desired blotting time and force were set on the cryo plunger for different types of samples.

3. After the blotting process, plunge-freeze the sample-loaded chip immediately in liquid ethane. Transfer the chip to the grid box in liquid nitrogen (LN_2) and store it in LN_2 before cryo-EM imaging.

2. Carry out cryo-EM imaging.
   1. Load the cryo-sample to a cryo-EM holder with the temperature maintained at -180 °C.
   2. Load the cryo-EM holder into a TEM and observe the samples with the minimum dose system (MDS) mode.

Representative Results

A micro-patterned chip with GO windows was fabricated by MEMS fabrication and 2D GO nanosheet transfer. Chips for micro-patterning were mass-produced, with about 500 chips produced from one 4 in wafer (**Figure 1B** and **Figure 2A,B**). The designs of the micro-patterned chips can be manipulated using different designs of the chromium mask (**Figure 2**) during the photolithography procedure. The fabricated micro-patterned chips had controlled numbers and dimensions of free-standing Si_xN_y membranes. The numbers of the free-standing Si_xN_y membranes were controlled from 48 (6 x 8) to 50 (5 x 10) and the dimensions from 50 x 40 μm^2 to 250 x 40 μm^2 (**Figure 3A,B,F,G**). Each free-standing Si_xN_y membrane can have tens to hundreds of micro-holes with customizable diameters ranging from 2-3 µm with different hole spacing. Fabricated micro-patterned chips have up to ~25,000 GO-suspended holes, while the number of the holes is also controllable (**Figure 3B-D** and **Figure 3G-I**). The existence of the thin GO layer across the hole was confirmed by Raman spectroscopy and electron diffraction. The Raman spectrum at the GO window showed representative peaks of GO, namely D and G bands at 1360 cm^{-1} and 1590 cm^{-1}, respectively[22] (**Figure 3E**). The multiply-oriented hexagonal diffraction patterns indicate that the windows consist of multilayer GO (**Figure 3J**).

The micro-patterned chip with GO windows was fabricated in three representative target depths (25 nm, 50 nm, and 100 nm) by controlling the deposition thickness of the Si_xN_y on the Si wafer during the LPCVD process to confirm the feasibility of regulating the depth of the micro-holes. To evaluate the structure and the thickness of the micro-holes with GO windows, 40°-tilted and cross-sectional scanning electron microscope (SEM) images and atomic force microscopy (AFM) images of the micro-patterned chip with GO windows were obtained. Well-type structure of the micro-hole with a GO window was clearly observed, with the depth of the micro-hole corresponding to the targeted depth (**Figure 4**). The results confirm that controlling the number and the design of the micro-patterned chip with GO windows is possible.

To demonstrate the use of the micro-patterned chip for cryo-EM imaging, various cryo-samples of biomolecules and inorganic NPs were prepared using the micro-patterned chip. For biological specimens, HIV-1, ferritin, proteasome 26S, groEL, apoferritin protein particles, and tau filament proteins were imaged with cryo-EM using the micro-patterned chip with GO windows (**Figure 5A-F**). Besides biomolecules, inorganic materials such as Fe_2O_3 NPs, Au NPs, Au

Copyright © 2022 JoVE Journal of Visualized Experiments

nanorods, and silica NPs were also observed by cryo-EM using micro-patterned chips (**Figure 5G-J**).

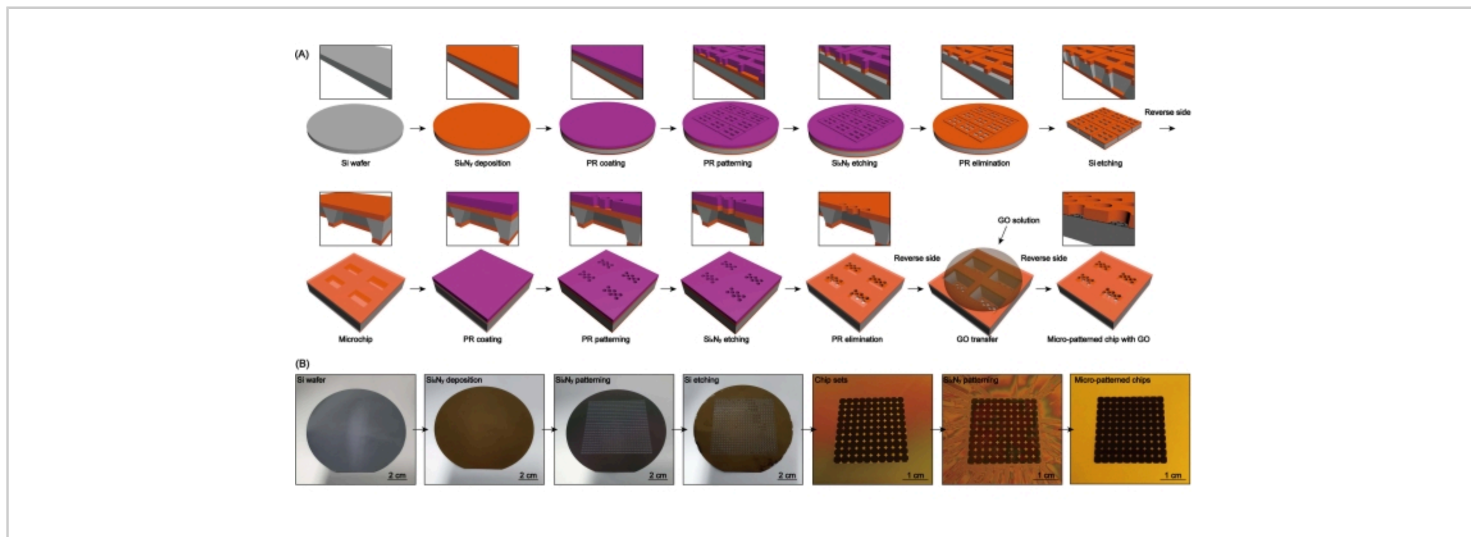

Figure 1: Schematics and images of the fabrication procedure of the newly developed micro-patterned chip with GO windows for cryo-EM. (**A**) Schematics of the fabrication process and cross-sections of the micro-patterned chip with GO windows during the fabrication process. (**B**) Images of the fabrication products at each fabrication step. Please click here to view a larger version of this figure.

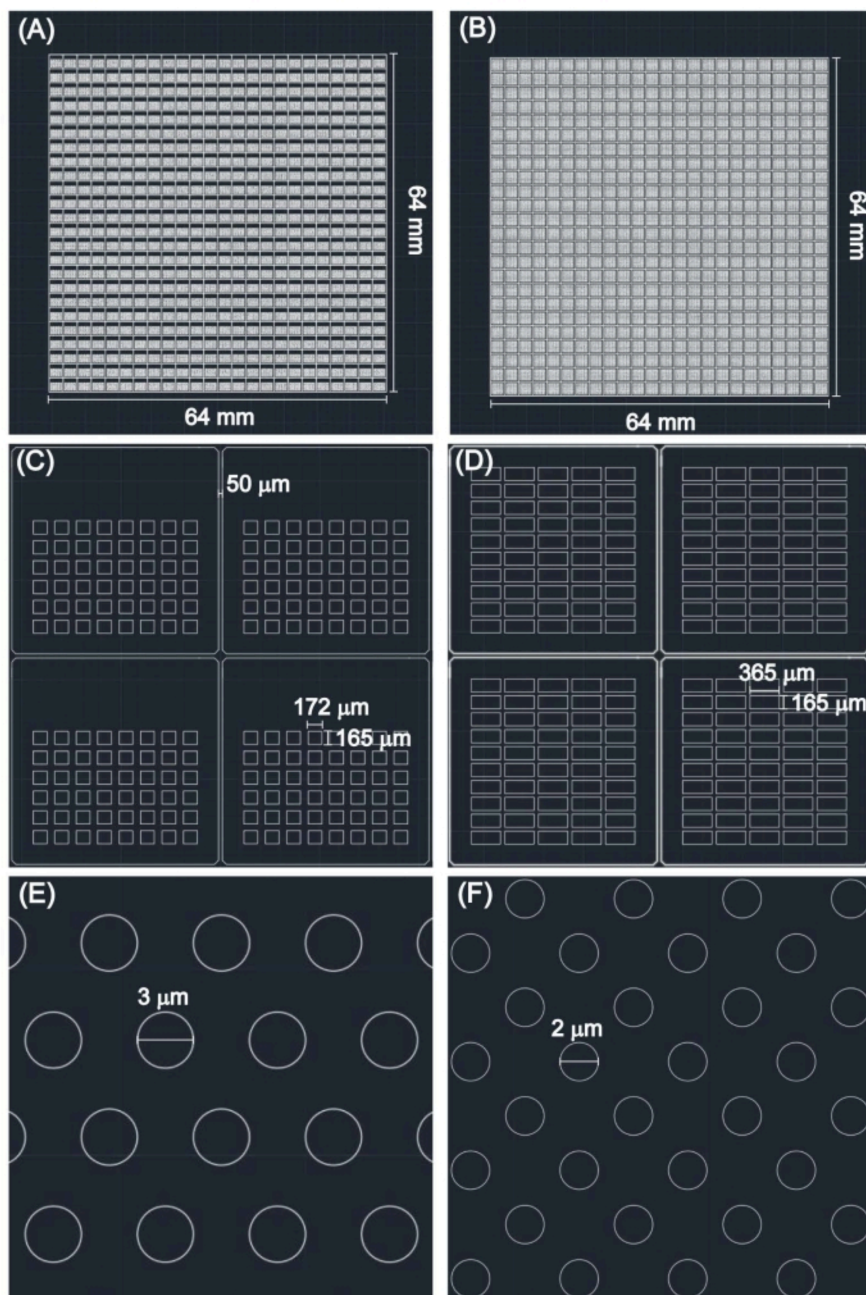

Figure 2: Brief illustration of the chromium masks used for the photolithography process. (**A,B**) Mask design for mass production of chips for a 4 in Si wafer (24 x 24 array of chips), (**C,D**) designs of 2 x 2 array of chips, and (**E,F**) designs of micro-hole patterns. Please click here to view a larger version of this figure.

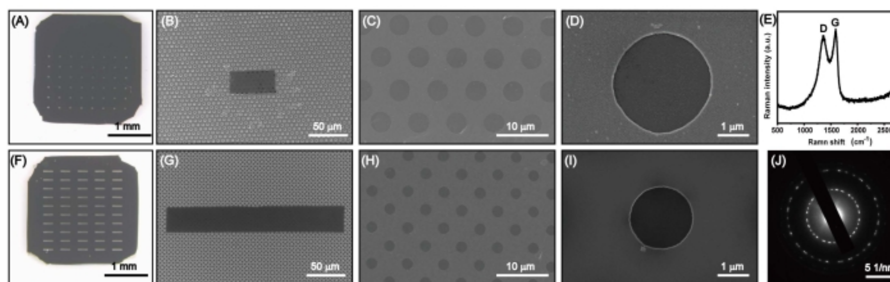

Figure 3: Structure of the micro-patterned chips with GO windows. (**A,F**) Optical microscopy images of whole micro-patterned chips, (**B,G**) SEM images of single micro-patterned Si_xN_y membranes, (**C,H**) SEM images of micro-patterns, and (**D,I**) SEM images of single micro-holes with GO windows. (**E,J**) Confirmation of GO at the micro-hole through (**E**) the Raman spectrum and (**J**) the selected area electron diffraction (SAED) pattern of the GO window. Please click here to view a larger version of this figure.

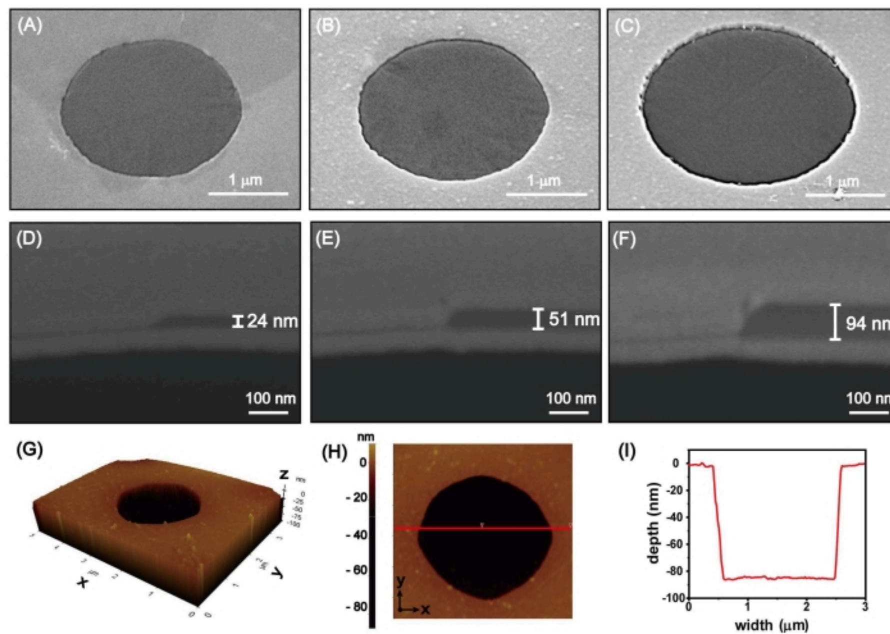

Figure 4: Well-structure and depth of the micro-hole with GO windows. (**A-C**) 40° tilted SEM images of a single micro-hole with a GO window, and (**D-F**) cross-sectional SEM image of the micro-patterned chip with GO windows in different depths (25 nm, 50 nm, and 100 nm). (**G**) Atomic force microscopy (AFM) 3D rendering image, (**H**) AFM deflection image, and (**I**) line profile along the red line in (**H**) showing the depth of the micro-patterned chip with GO windows fabricated with 100 nm Si_xN_y membrane. Please click here to view a larger version of this figure.

Copyright © 2022 JoVE Journal of Visualized Experiments

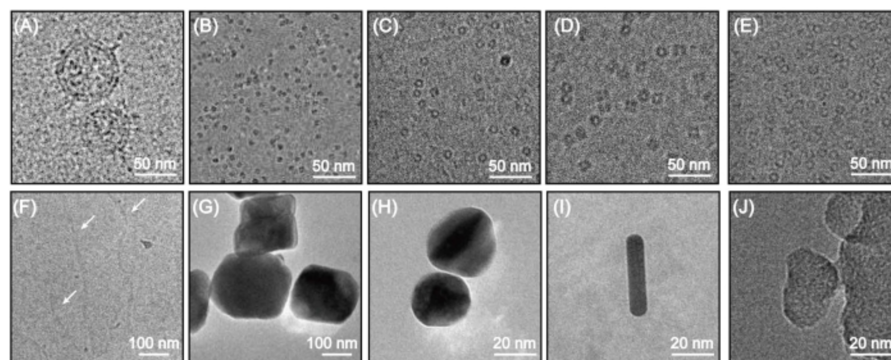

Figure 5: Cryo-EM images of various sized biomaterials and inorganic nanomaterials using the micro-patterned chip with GO windows. (**A**) HIV-1 virus particle, (**B**) ferritin, (**C**) proteasome 26S, (**D**) groEL, (**E**) apoferritin, (**F**) tau protein (arrows indicating fibrillized tau protein), (**G**) Fe_2O_3 NP, (**H**) Au NP, (**I**) Au nanorod, and (**J**) silica NP. Please click here to view a larger version of this figure.

Discussion

The microfabrication processes for producing micro-patterned chips with GO windows are introduced here. The fabricated micro-patterned chip is designed to regulate the thickness of the vitreous ice layer by controlling the depth of the micro-hole with GO windows depending on the size of the material to be analyzed. A micro-patterned chip with GO windows was fabricated using a series of MEMS techniques and a 2D nanosheet transfer method (**Figure 1**). The major advantage of using the MEMS fabrication technique is its capability for mass production and the feasibility of manipulating the structure and dimensions of the microchip by using different designs of the chromium mask during photolithography (**Figure 2**). The LPCVD-deposited Si_xN_y layer with low stress ensures the stability of the tens of nanometers thick free-standing Si_xN_y[23,24,25,26]. However, the nanometer-scale free-standing Si_xN_y layer is still vulnerable to forces in the perpendicular direction[27]. Therefore, extreme caution is needed while handling the micro-patterned chip, such as when dipping in solution or blow-drying. In addition, the fabrication process for the micro-patterned chip uses the 100 µm Si wafer, which ensures compatibility with most cryo-EM specimen holders and autoloaders. However, caution is needed during the fabrication processes to prevent the fragile wafer from fracturing.

The micron-scale regular array of well-type structures with GO windows was confirmed with an optical microscope and an SEM (**Figure 3** and **Figure 4**). Besides, the drop casting method for transferring GO enables GO deposition with high flatness and without noticeable wrinkles (**Figure 3D,E,I,J**). The micro-patterned chip is suitable for loading in the cryo-EM autoloader, and tens of thousands of micron-scale holes in a regular array allow the automated collection of large image data for single particle analysis. Moreover, the number and the morphology of Si_xN_y membranes and GO-supported micro-holes can be manipulated easily in the MEMS fabrication process,

allowing for high-throughput single particle analysis and other cryo-EM imaging experiments depending on the research purposes. Furthermore, extended applications of micro-patterned chips with controlled thickness can be facilitated by the fabrication of chips that have holes patterned at the nanometer scale. Nano-patterning techniques developed in the semiconductor industry can be adopted in the fabrication of those chips[28,29,30].

The capability of regulating the depth of the micro-holes has been demonstrated here by fabricating micro-patterned chips with GO windows in three representative target depths: 25 nm, 50 nm, and 100 nm. Different depths of the microwell structure were achieved by controlling the deposition time of the Si_xN_y layer on the Si wafer (**Figure 4**). For evaluating the morphology and the thickness of the micro-patterned chip with GO windows, cross-sections of the devices obtained from focused ion beam (FIB) sectioning were observed with SEM, and the depth profile was measured with AFM (**Figure 4**). The well-type structure of the micro-hole with GO window was clearly shown in the SEM and AFM images, confirming successful control of the depth of the Si_xN_y micro-hole and transfer of the GO window. The use of the customizable micro-patterned chip with GO windows is likely to ensure a high success rate in producing regions of optimal ice thickness for cryo-EM imaging.

Since the materials to be observed with cryo-EM have different sizes, producing vitreous ice with an appropriate thickness can ensure enhanced contrast resolution, a wide orientation coverage, and reduced denaturation of the structure during cryo-EM imaging. To demonstrate the use of the cryo-EM imaging process for biological applications, various biological samples of different sizes, including HIV-1, ferritin, proteasome 26S, groEL, apoferritin, and tau protein, were imaged using the micro-patterned chip with GO windows. The biomolecules were clearly observed using the micro-patterned chip with GO windows (**Figure 5A-F**). Besides biomolecules, diverse types of inorganic nanomaterials, such as Fe_2O_3 NPs, Au NPs, Au nanorods, and silica NPs, were also observed using the micro-patterned chip with GO windows (**Figure 5G-J**). The micro-patterned chip and fabrication method show compatibility for the cryo-imaging of various materials. Thus, the newly developed micro-patterned chip with GO windows provides a reliable and reproducible sample preparation strategy for efficient and high-throughput structure analysis with cryo-EM.

Disclosures

The authors have no conflicts of interest.

Acknowledgments

M.-H.K., S.K., M.L., and J.P. acknowledge the financial support from the Institute for Basic Science (Grant No. IBS-R006-D1). S.K., M.L., and J.P. acknowledge the financial support from Creative-Pioneering Researchers Program through Seoul National University (2021) and the NRF grant funded by the Korean government (MSIT; Grant Nos. NRF-2020R1A2C2101871, and NRF-2021M3A9I4022936). M.L. and J.P. acknowledge the financial support from the POSCO Science Fellowship of POSCO TJ Park Foundation and the NRF grant funded by the Korean government (MSIT; Grant No. NRF-2017R1A5A1015365). J.P. acknowledges the financial support from the NRF grant funded by the Korean government (MSIT; Grant No. NRF-2020R1A6C101A183), and the Interdisciplinary Research Initiatives Programs by College of Engineering and College of Medicine, Seoul National University (2021). M.-H.K. acknowledges the financial support from the NRF

Copyright © 2022 JoVE Journal of Visualized Experiments

grant funded by the Korean government (MSIT; Grant No. NRF-2020R1I1A1A0107416612). The authors thank the staff and crew of the Seoul National University Center for Macromolecular and Cell Imaging (SNU CMCI) for their untiring efforts and perseverance with the cryo-EM experiments. The authors thank S. J. Kim of the National Center for Inter-university Research Facilities for assistance with the FIB-SEM experiments.

References

1. Dillard, R. S. et al. Biological applications at the cutting edge of cryo-electron microscopy. *Microscopy and Microanalysis.* **24** (4), 406-419 (2018).
2. Meyerson, J. R. et al. Self-assembled monolayers improve protein distribution on holey carbon cryo-EM supports. *Scientific Reports.* **4** (2014).
3. Palovcak, E. et al. A simple and robust procedure for preparing graphene-oxide cryo-EM grids. *Journal of Structural Biology.* **204** (1), 80-84 (2018).
4. Xu, B. J., Liu, L. Developments, applications, and prospects of cryo-electron microscopy. *Protein Science.* **29** (4), 872-882 (2020).
5. Stewart, P. L. Cryo-electron microscopy and cryo-electron tomography of nanoparticles. *Wiley Interdisciplinary Reviews-Nanomedicine and Nanobiotechnology.* **9** (2) (2017).
6. Murata, K., Wolf, M. Cryo-electron microscopy for structural analysis of dynamic biological macromolecules. *Biochimica Et Biophysica Acta-General Subjects.* **1862** (2), 324-334 (2018).
7. Darrow, M. C. et al. Chameleon: next generation sample preparation for cryoEM based on spotiton. *Acta Crystallographica a-Foundation and Advances.* **75**, A424-A424 (2019).
8. Hite, R. K., Tao, X., MacKinnon, R. Structural basis for gating the high-conductance Ca2+-activated K+ channel. *Nature.* **541** (7635), 52-57 (2017).
9. Zhang, Y. et al. Cryo-EM structure of the activated GLP-1 receptor in complex with a G protein. *Nature.* **546** (7657), 248-253 (2017).
10. Shaik, M. M. et al. Structural basis of coreceptor recognition by HIV-1 envelope spike. *Nature.* **565** (7739), 318-323 (2019).
11. Liu, C. et al. The architecture of inactivated SARS-CoV-2 with postfusion spikes revealed by cryo-EM and cryo-ET. *Structure.* **28** (11), 1218-1224 (2020).
12. Ren, X. C., Zhang, X. Q., Xu, R., Huang, J. Q., Zhang, Q. Analyzing energy materials by cryogenic electron microscopy. *Advanced Materials.* **32** (24), 1908293 (2020).
13. Li, Y. Z. et al. Atomic structure of sensitive battery materials and Interfaces revealed by cryo-electron microscopy. *Science.* **358** (6362), 506-510 (2017).
14. Li, Y. B., Huang, W., Li, Y. Z., Chiu, W., Cui, Y. Opportunities for cryogenic electron microscopy in materials science and nanoscience. *Acs Nano.* **14** (8), 9263-9276 (2020).
15. Kim, Y. et al. Uniform synthesis of palladium species confined in a small-pore zeolite via full ion-exchange investigated by cryogenic electron microscopy. *Journal of Materials Chemistry A.* **9** (35), 19796-19806 (2021).
16. Baumgartner, J. et al. Nucleation and growth of magnetite from solution. *Nature Materials.* **12** (4), 310-314 (2013).

Copyright © 2022 JoVE Journal of Visualized Experiments

17. Rice, W. J. et al. Routine determination of ice thickness for cryo-EM grids. *Journal of Structural Biology.* **204** (1), 38-44 (2018).
18. D'Imprima, E. et al. Protein denaturation at the air-water interface and how to prevent it. *Elife.* **8**, e42747 (2019).
19. Alden, N. A. et al. Cryo-EM-on-a-chip: custom-designed substrates for the 3D analysis of macromolecules. *Small.* **15** (21), e1900918 (2019).
20. Naydenova, K., Peet, M. J., Russo, C. J. Multifunctional graphene supports for electron cryomicroscopy. *Proceedings of the National Academy of Sciences of the United States of America.* **116** (24), 11718-11724 (2019).
21. Kang, M. H. et al. Graphene oxide-supported microwell grids for preparing cryo-EM samples with controlled ice thickness. *Advanced Materials.* **33** (43), 2102991 (2021).
22. Johra, F. T., Lee, J. W., Jung, W. G. Facile and safe graphene preparation on solution based platform. *Journal of Industrial and Engineering Chemistry.* **20** (5), 2883-2887 (2014).
23. Yang, C., Pham, J. Characteristic study of silicon nitride films deposited by LPCVD and PECVD. *Silicon.* **10** (6), 2561-2567 (2018).
24. Olson, J. M. Analysis of LPCVD process conditions for the deposition of low stress silicon nitride. Part I: preliminary LPCVD experiments. *Materials Science in Semiconductor Processing.* **5** (1), 51-60 (2002).
25. Zheng, B. R., Zhou, C., Wang, Q., Chen, Y. F., Xue, W. Deposition of low stress silicon nitride thin film and its application in surface micromachining device structures. *Advances in Materials Science and Engineering.* **2013**, 835942 (2013).
26. Chuang, W. H., Fettig, R. K., Ghodssi, R. An electrostatic actuator for fatigue testing of low-stress LPCVD silicon nitride thin films. *Sensors and Actuators a-Physical.* **121** (2), 557-565 (2005).
27. Shafikov, A. et al. Strengthening ultrathin Si3N4 membranes by compressive surface stress. *Sensors and Actuators a-Physical.* **317**, 112456 (2021).
28. Ng, W. H. et al. Controlling and modelling the wetting properties of III-V semiconductor surfaces using re-entrant nanostructures. *Scientific Reports.* **8**, 3544 (2018).
29. Han, D. et al. Nanopore-templated silver nanoparticle arrays photopolymerized in zero-mode waveguides. *Frontiers in Chemistry.* **7**, 216 (2019).
30. Escobedo, C. On-chip nanohole array based sensing: a review. *Lab Chip.* **13**, 2445-2463 (2013).

Copyright © 2022 JoVE Journal of Visualized Experiments